

# Decoherence of Einstein-Podolsky-Rosen steering

L. Rosales-Zárata, R. Y. Teh, S. Kiesewetter, A. Brolis, K. Ng and M. D. Reid<sup>1</sup>

<sup>1</sup>Centre for Quantum and Optical Science, Swinburne University of Technology, Melbourne, 3122 Australia

We consider two systems  $A$  and  $B$  that share Einstein-Podolsky-Rosen (EPR) steering correlations and study how these correlations will decay, when each of the systems are independently coupled to a reservoir. EPR steering is a directional form of entanglement, and the measure of steering can change depending on whether the system  $A$  is steered by  $B$ , or vice versa. First, we examine the decay of the steering correlations of the two-mode squeezed state. We find that if the system  $B$  is coupled to a reservoir, then the decoherence of the steering of  $A$  by  $B$  is particularly marked, to the extent that there is a sudden death of steering after a finite time. We find a different directional effect, if the reservoirs are thermally excited. Second, we study the decoherence of the steering of a Schrodinger cat state, modelled as the entangled state of a spin and harmonic oscillator, when the macroscopic system (the cat) is coupled to a reservoir.

OCIS: 270.0270; 270.6570; 270.5568

## I. INTRODUCTION

The sort of nonlocality we call “Einstein-Podolsky-Rosen-steering” [1–6] originated in 1935 with the Einstein-Podolsky-Rosen (EPR) paradox [7]. The EPR paradox is the argument that was put forward by Einstein, Podolsky and Rosen for the incompleteness of quantum mechanics. The argument was based on premises (sometimes called *Local Realism* or in Einstein’s language, no “spooky action-at-a-distance”) that were not restricted to classical mechanics, but were thought essential to any physical theory [8]. The EPR argument reveals the inconsistency between Local Realism and the completeness of quantum mechanics. It does not in itself rule out all completions of quantum mechanics, that are compatible with local realism. Nowadays, after the work of Bell, we realise this ruling out of all local realistic theories can be done in some special experimental situations [9–12]. Any realisation of the EPR paradox [13–15], as a special case of EPR steering, is nonetheless important in giving a concrete intermediate result: the fact that quantum mechanics without completion cannot be consistent with local realism. A great advantage of EPR-steering over Bell-type tests is that they are more accessible to mesoscopic or macroscopic systems. EPR steering tests have been quantitatively studied or proposed for optical down conversion [14–17], optical systems in nonlinear regimes near or at critical points [18], atomic gas ensembles at room temperature [19–21], Bose-Einstein condensates (BEC) [22–31], and opto-mechanics [32–35]. This may lead to experimental tests of Schrodinger cat-type states.

The EPR paradox manifests as a strong correlation between the positions and momenta of two spatially separated particles (or some equivalent correlations). These correlations, once one assumes Local Realism, become inconsistent with the uncertainty principle. Given the strangeness of the EPR correlations, a likely hypothesis would be that they do not exist in real physical systems. Indeed, the sort of correlations needed for EPR are not easily realisable in experiment. To date, only a few

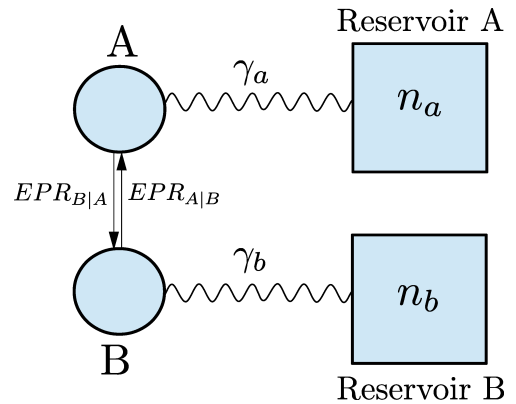


Figure 1. Our question is this: We consider two well-separated systems,  $A$  and  $B$ , that possess the type of quantum correlation we call EPR-steering. Each system is independently coupled to a thermal reservoir, at a time  $t = 0$ . This coupling induces a decay of the EPR-steering. We ask how does the decay of the steering depend on: the coupling  $\gamma_a, \gamma_b$  to each reservoir; the thermal excitation  $n_a, n_b$  of each reservoir; and the measure that gives the strength of the EPR-steering. We will consider two types of EPR systems: The first is a two-mode squeezed state. The second is a mesoscopic/ macroscopic entangled “Schrodinger cat” state.

experiments can justify the claim of loophole-free EPR correlations [36], or steering without detection efficiency loopholes [14, 15, 37, 38]. This paper examines why this is so: There are two possibilities.

(1) It could be that quantum mechanics needs modification to the extent that EPR correlations cannot be predicted. If we accept irrefutable evidence now exists for EPR correlations, then this probability would appear falsified. However, we comment that the experimental realisations for EPR steering have been for optical systems, not yet for atoms or mesoscopic devices.

(2) Or else: a popular belief is that quantum mechanics is correct as it is, and predicts exactly why, to a great accuracy, the EPR correlations are extraordinarily difficult to measure. In that case, these predictions need to be evaluated and verified by experiment.

This last point is what we examine in this paper: We study in detail why, according to quantum predictions, the EPR correlations are not easily realisable. As with the well known ‘‘Schrodinger cat’’ [39–48], we expect this is so, because of the effect that occurs when a quantum system is coupled to its environment, modelled as a large system - a reservoir [49]. This effect is called ‘‘decoherence’’.

Here, we examine some different sorts of decoherence that occur for EPR steering. As with the decay of entanglement, there are many cases one can study. It is worth noting that EPR steering was realised using high efficiency detection for optical amplitudes [14, 15], and has also been unambiguously detected in photonic scenarios with exceptional losses ( $\sim 87\%$ ) [38]. Tests have also begun for its genuine multipartite form, distributed among different locations [50–53].

In this paper, we restrict our investigation to the following cases: We study position-momentum measurements or their optical equivalent, quadrature phase amplitude measurements. First, we analyze the steering of a two-mode squeezed state, to understand the decoherence effects of coupling to a thermal reservoir. We examine two properties of the decoherence: the effect of simple losses (damping); and the effect of thermal noise. Second, we consider a special case of EPR-steering, that relates to a macroscopic/mesoscopic superposition state - a ‘‘Schrodinger cat’’ state. In fact, the EPR-steering paradox can be used to signify the Schrodinger cat superposition [54]. We examine the effect of decoherence as caused by interaction with the environment, on this signature.

An interesting new feature evident for EPR-steering is that the nonlocality can manifest *asymmetrically* with respect to the observers [55–60]. In our results, we focus on the asymmetry of the decoherence effects on the EPR-steering. This is valuable to understand, not only from the fundamental perspective of testing quantum mechanics, but from the point of view of the potential applications of EPR-steering, which include cryptography [61–66] and no-cloning teleportation [65]. One-sided device-independent cryptography has been proposed using EPR steering inequalities [64]. In recent papers, it was shown how the asymmetric effects of loss on EPR-steering could affect the optimal location of teleportation stations [67], or which entanglement criterion should be used to faithfully verify entanglement in cases of untrusted devices [64–68].

## II. DECOHERENCE OF STEERING FOR THE TWO-MODE SQUEEZED STATE

Consider two quantum harmonic oscillators, with boson operators  $a$  and  $b$ , and depicted in the Figure 1 as systems  $A$  and  $B$ . Such oscillators can be coupled, so that EPR-steering correlations are induced between the two oscillators.

One of the nicest examples of such EPR steering has been realised experimentally in optics [15] as the two-mode squeezed state [69]. Here, each mode of the light field is modeled as a quantum harmonic oscillator. An example of a coupling between the oscillators that generates this type of state is called parametric down conversion, and can be described by the interaction Hamiltonian in an appropriate rotating frame [16]

$$H = i\kappa E(ab - a^\dagger b^\dagger) \quad (1)$$

Similar two-mode squeezed states can be generated by impinging two single-mode squeezed states into the two different input ports of an optical beam splitter [70].

The two-mode squeezed state system is fundamentally interesting, as it can be quite accurately realised in optics, but also it gives a reasonable approximation to the effects we expect to see in many other physical realisations of steering, such as in opto-mechanics [32, 34, 35], atomic ensembles [19–21], and BEC [22–30]. The study of the effect of the thermal environment on the EPR steering for a two-mode squeezed state will therefore give us insight into a broad set of physical scenarios. The two-mode quantum correlation effects were noticed originally in the context of photon number correlations between the two beams, which gives rise to noise reduction [71, 72].

### A. The two-mode squeezing Hamiltonian

We begin by reviewing the solution for the EPR correlations given by the Hamiltonian of Eq. (1). The EPR solutions were originally derived in [16]. We define the quadrature phase amplitudes  $X_A$ ,  $P_A$ ,  $X_B$  and  $P_B$  for each mode:  $X_A = a + a^\dagger$ ,  $P_A = (a - a^\dagger)/i$  and  $X_B = b + b^\dagger$ ,  $P_B = (b - b^\dagger)/i$ . This choice of scaling for the amplitudes will imply the Heisenberg uncertainty relations  $\Delta X_A \Delta P_A \geq 1$  and  $\Delta X_B \Delta P_B \geq 1$ . We note that depending on the physical system modelled by the Hamiltonian, the amplitudes can also correspond to scaled position and momentum observables. We now ask what correlations are generated between the quadrature amplitudes, after an interaction time  $\tau$  between the two modes, at sites denoted by  $A$  and  $B$ .

On examining (1), the resulting coupled equations for  $a$  and  $b$  can be readily solved, to give

$$\begin{aligned} a(\tau) &= \eta a(0) - \sqrt{(\eta^2 - 1)} b^\dagger(0) \\ b(\tau) &= \eta b(0) - \sqrt{(\eta^2 - 1)} a^\dagger(0) \end{aligned} \quad (2)$$

where  $\eta = \cosh r$ . We define the squeezing parameter as  $r = \frac{E\kappa}{\hbar}\tau$ . The quadrature phase amplitudes are given by

$$\begin{aligned} X_A(\tau) &= \cosh r X_A(0) - \sinh r X_B(0) \\ P_A(\tau) &= \cosh r P_A(0) + \sinh r P_B(0) \\ X_B(\tau) &= \cosh r X_B(0) - \sinh r X_A(0) \\ P_B(\tau) &= \cosh r P_B(0) + \sinh r P_A(0) \end{aligned} \quad (3)$$

This enables us to calculate correlations such as  $\langle X_A^2 \rangle$ ,  $\langle X_A X_B \rangle$  after a time  $\tau$ , assuming initial uncorrelated

vacuum states for all modes. We can then evaluate the variance of  $X_A - g_x X_B$ , which will be denoted  $\Delta^2(X_A - g_x X_B)$  and which equals  $\langle (X_A - g_x X_B)^2 \rangle$  when we assume vacuum inputs at  $\tau = 0$ . We have introduced constants  $g_x$ , which can be chosen to minimise the variance relative to the Heisenberg quantum noise level of the amplitudes  $X_A$  and  $P_A$ . We find this value of  $g_x$  by standard procedures [15, 16]:

$$\frac{\partial}{\partial g_x} \Delta^2(X_A - g_x X_B) = 0, \quad \Leftrightarrow g_x = \frac{\langle X_A X_B \rangle}{\langle X_B^2 \rangle} \quad (4)$$

For the system described by the Hamiltonian of Eq. (1), we find the optimal value is  $g_x = -\tanh 2r$ . The optimal variance is given by:

$$\Delta^2(X_A - g_x X_B) = \langle X_A^2 \rangle - \frac{\langle X_A X_B \rangle^2}{\langle X_B^2 \rangle} \quad (5)$$

which for the parametric system (1) becomes  $\Delta^2(X_A - g_x X_B) = \frac{1}{\cosh 2r}$ . Similarly we evaluate the variance of  $P_A + g_p P_B$ , which we will denote as  $\Delta^2(P_A + g_p P_B)$ : The variance minimizes when

$$\frac{\partial}{\partial g_p} \Delta^2(P_A + g_p P_B) = 0, \quad \Leftrightarrow g_p = -\frac{\langle P_A P_B \rangle}{\langle P_B^2 \rangle}$$

This optimal value of  $g_p$  for system (1) is  $g_p = -\tanh 2r$ . The optimal variance is given by

$$\Delta^2(P_A + g_p P_B) = \langle P_A^2 \rangle - \frac{\langle P_A P_B \rangle^2}{\langle P_B^2 \rangle} \quad (6)$$

which becomes  $\Delta^2(P_A + g_p P_B) = \frac{1}{\cosh 2r}$  for Eq. (1).

## B. EPR steering correlations

The criterion for the EPR paradox introduced in [16] is also a criterion for EPR steering [3–5]. This EPR steering criterion is defined as the square root of the variance product:

$$EPR_{A|B}(g_x, g_p) = \Delta(X_A - g_x X_B) \Delta(P_A + g_p P_B) \quad (7)$$

We observe EPR steering (of system  $A$  by  $B$ ) whenever

$$EPR_{A|B}(g_x, g_p) < 1 \quad (8)$$

The ideal correlations created by the parametric down conversion Hamiltonian interaction (1) are obtained in the limit of  $r \rightarrow \infty$  and correspond to the EPR variances becoming zero, and hence  $EPR \rightarrow 0$ .

The EPR steering condition (8) by its very definition will negate all *local hidden state* (LHS) models of the type [3, 4]

$$\langle X_A^\theta X_B^\phi \rangle \equiv \langle \hat{X}_A^\theta X_B^\phi \rangle = \int P(\lambda) \langle X_A^\theta \rangle_\lambda \langle X_B^\phi \rangle_\lambda d\lambda \quad (9)$$

These LHS models are similar to the local hidden variable models introduced by Bell [9, 10]. Here  $\lambda$  represents hidden variable parameters and  $P(\lambda)$  is the probability distribution for these parameters. The  $P(\lambda)$  is independent of the choice of measurement ( $\theta$  and  $\phi$ ), which is made *after* the generation and separation of the subsystems  $A$  and  $B$ . In this model, the  $\langle X_A^\theta \rangle_\lambda$  is the average value for the result  $X_A^\theta$ , given the hidden variable state specified by  $\lambda$ . The  $\langle X_B^\phi \rangle_\lambda$  is defined similarly. For the LHS model however, there is the additional *asymmetrical* constraint that the *local* hidden variable moments (such as  $\langle X_A^\theta \rangle_\lambda$ ) for system  $A$  be consistent with measurements of some local observables (for example position and momentum) at  $A$ , and is thus able to be described as arising from a local *quantum* density operator  $\rho_A^\lambda$ .

We can define the minimum value of  $EPR$  after optimising  $g_x$  and  $g_p$  as:  $EPR_{A|B} = \min\{EPR_{A|B}(g_x, g_p)\}$ . Thus, for the Hamiltonian of Eq. (1):

$$EPR_{A|B} = \frac{1}{\cosh 2r} \quad (10)$$

as derived originally in [16]. Ideal EPR correlations are obtained as  $r \rightarrow \infty$ , in which case  $EPR_{A|B} \rightarrow 0$ , and we say the “steering is perfect”.

## C. Reservoir coupling

We now examine the effect on EPR steering if the systems  $A$  and  $B$  are independently coupled to heat bath reservoirs (Figure 1). We assume that the parametric interaction  $H$  given by (1) that generates a two-mode squeezed state is turned off at the time  $t = 0$ , and the system left to decay. The two-mode squeezed state is a so-called Gaussian state, meaning that its characteristic function is Gaussian [73]. Within the constraint of two-mode Gaussian states and measurements, the condition (8) will provide a *necessary and sufficient* test of steering [3, 4]. This makes the criterion valuable, for understanding the effects of decoherence in Gaussian systems.

Thus, we consider a system *prepared* in a two-mode squeezed state at time  $t = 0$ . In principle, the modes  $a$  and  $b$  can be spatially separated. We consider the coupling of each mode  $a$  and  $b$  to independent heat baths (reservoirs) with thermal occupation numbers  $n_a$  and  $n_b$  respectively. The solutions after coupling to the reservoir are straightforward to evaluate using the operator Langevin equations that describe the evolution of the mode operators [74, 75]:

$$\begin{aligned} \dot{a} &= -\gamma_a a + \sqrt{2\gamma_a} \Gamma_a(t) \\ \dot{b} &= -\gamma_b b + \sqrt{2\gamma_b} \Gamma_b(t) \end{aligned} \quad (11)$$

Here  $\gamma_a$  and  $\gamma_b$  describe the decay rates (losses) that are induced by the reservoirs. The quantum reservoir operators  $\Gamma(t)$  have nonzero correlations given by  $\langle \Gamma_a^\dagger(t) \Gamma_a(t') \rangle = n_a \delta(t - t')$  and  $\langle \Gamma_a(t) \Gamma_a^\dagger(t') \rangle = (n_a +$

1) $\delta(t-t')$  where the numbers  $n_a$  and  $n_b$  give the level of thermal occupation of the reservoirs. Solutions are

$$a(t) = e^{-\gamma_a t} a(0) + \sqrt{2\gamma_a} \int_0^t e^{-\gamma_a(t-t')} \Gamma_a(t') dt' \quad (12)$$

From this, we can calculate the moments at a later time, in terms of the initial moments:

$$\begin{aligned} \langle a^\dagger(t)a(t) \rangle &= e^{-2\gamma_a t} \langle a^\dagger(0)a(0) \rangle + n_a(1 - e^{-2\gamma_a t}) \\ \langle a(t)b(t) \rangle &= e^{-(\gamma_a+\gamma_b)t} \langle a(0)b(0) \rangle \end{aligned} \quad (13)$$

The solution for  $\langle b^\dagger(t)b(t) \rangle$  is obtained from that for  $\langle a^\dagger(t)a(t) \rangle$ , but exchanging the letters  $a$  with  $b$ . The initial moments are given by the solutions found in Section

II.A. The final moments after reservoir coupling are

$$\begin{aligned} \langle a^\dagger(t)a(t) \rangle &= n_a(1 - e^{-2t\gamma_a}) + e^{-2t\gamma_a} \sinh^2(r) \\ \langle a(t)b(t) \rangle &= -e^{-(\gamma_a+\gamma_b)t} \cosh r \sinh r \end{aligned} \quad (14)$$

The covariance matrix  $V$  is defined as:

$$V = \begin{bmatrix} \langle X_A^2 \rangle & \langle X_A P_A \rangle & \langle X_A X_B \rangle & \langle X_A P_B \rangle \\ \langle P_A X_A \rangle & \langle P_A^2 \rangle & \langle P_A X_B \rangle & \langle P_A P_B \rangle \\ \langle X_B X_A \rangle & \langle X_B P_A \rangle & \langle X_B^2 \rangle & \langle X_B P_B \rangle \\ \langle P_B X_A \rangle & \langle P_B P_A \rangle & \langle P_B X_B \rangle & \langle P_B^2 \rangle \end{bmatrix} \quad (15)$$

Hence we find  $V_{14} = V_{23} = 0$ ,  $V_{12} = V_{34} = i$ ,  $V_{11} = V_{22}$ ,  $V_{33} = V_{44}$ ,  $V_{24} = -V_{13}$  where

$$\begin{aligned} V_{11} &= e^{-2\gamma_a t} \cosh 2r + (1 - e^{-2\gamma_a t})(1 + 2n_a) \\ V_{33} &= e^{-2\gamma_b t} \cosh 2r + (1 - e^{-2\gamma_b t})(1 + 2n_b) \\ V_{24} &= e^{-(\gamma_a+\gamma_b)t} \sinh 2r \end{aligned} \quad (16)$$

Applying the results of the Section II.A, we calculate that

$$EPR_{A|B} = \frac{\cosh 2r [e^{-2\gamma_a t} (1 - e^{-2\gamma_b t})(1 + 2n_b) + e^{-2\gamma_b t} (1 - e^{-2\gamma_a t})(1 + 2n_a)] + e^{-2(\gamma_a+\gamma_b)t} + (1 + 2n_a)(1 + 2n_b)(1 - e^{-2\gamma_b t})(1 - e^{-2\gamma_a t})}{e^{-2\gamma_b t} \cosh 2r + (1 - e^{-2\gamma_b t})(1 + 2n_b)} \quad (17)$$

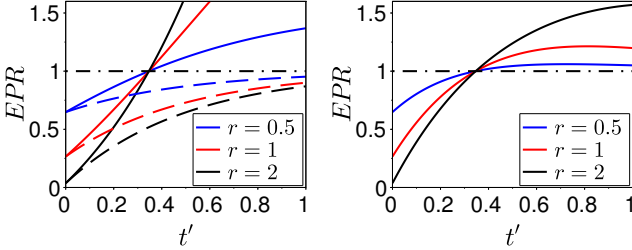


Figure 2. The decoherence of two-mode EPR steering with no thermal excitation ( $n_a = n_b = 0$ ). A sudden-death type of decoherence is noted when it is the system “doing the steering” that is coupled to the reservoir. The steering signatures  $EPR_{A|B}$  and  $EPR_{B|A}$  are plotted versus  $t' = \gamma_b t$ , for various values of squeeze parameter  $r$ . EPR steering is obtained for the Gaussian system iff  $EPR < 1$  and the strongest steering is when  $EPR \rightarrow 0$ . **Left graph:** Reservoir coupling to system  $B$  only ( $\gamma_a = 0$ ). Solid lines correspond to  $EPR_{A|B}$  while dashed lines correspond to  $EPR_{B|A}$ . Curves are (bottom to top on the far left)  $r = 2$  (black),  $r = 1$  (red),  $r = 0.5$  (blue). **Right graph:** Plots of  $EPR_{A|B}$  for symmetric coupling to the reservoirs:  $\gamma_a = \gamma_b$ . In this case,  $EPR_{A|B} = EPR_{B|A}$ .

#### D. Decoherence of EPR steering with no thermal noise

We first assume negligible thermal noises: we put  $n_a = n_b = 0$  in the solution given by Eq. (17). The decoherence effect on the system by the reservoirs manifests as losses, parametrised by  $\gamma_a$  and  $\gamma_b$ . We will study the effect on the steering parameters, showing the effect

of loss to be asymmetrical with respect to the two systems  $A$  and  $B$ .

##### 1. Damping the steering system: Steering sudden-death

Let us suppose that the reservoirs are coupled *asymmetrically*, so that  $\gamma_a \rightarrow 0$  i.e. only the mode  $b$  is coupled to a reservoir. In this case, we find for the steering of  $A$  (mode  $a$ )

$$EPR_{A|B} = \frac{e^{-2\gamma_b t} + \cosh 2r [1 - e^{-2\gamma_b t}]}{1 + e^{-2\gamma_b t} (\cosh 2r - 1)} \quad (18)$$

The plots of Figure 2 (left graph) indicate that where the losses are entirely on the steering mode  $B$ , the decoherence of EPR steering is substantial. After a time given by  $\gamma_b t = \frac{\ln 2}{2}$ , steering (as measured by  $EPR_{A|B}$ ) in that direction is lost. The loss is inevitable, regardless of how much steering is present in the initial two-mode quantum system, as shown by the results for the different values of squeeze parameter  $r$ : We also note that the *cut-off time* for steering is independent of the amount of steering  $r$  in the initial two-mode system. The behavior observed here is analogous to the “entanglement sudden-death”, that has been observed for the decoherence of entanglement [76–78].

##### 2. Damping the steered system

However, the sudden-death effect is not apparent when the “steered” system is lossy. We again assume  $\gamma_a \rightarrow 0$

and evaluate the steering of the damped system, by the undamped system:

$$EPR_{B|A} = \frac{e^{-2\gamma_b t} + \cosh 2r [1 - e^{-2\gamma_b t}]}{\cosh 2r} \quad (19)$$

The plots of Figure 2 (left graph) reveal the nature of the decoherence when only the steered system is damped. Here, we see that there is much less sensitivity of the steering to the losses. In fact, while the EPR steering is certainly diminished by the dissipation, there is no cut-off, or sudden death, but rather steering is still possible for arbitrary times,  $t \rightarrow \infty$ . We remark that the increased sensitivity to losses affecting the steering system, as compared to the steered system, has been noted in earlier papers [15, 55, 56, 59].

### 3. Symmetric decoherence

We next consider a reservoir with symmetric damping  $\gamma_a = \gamma_b$ .

$$EPR_{A|B} = \frac{e^{-4\gamma_b t} + (1 - e^{-2\gamma_b t})^2}{1 + e^{-2\gamma_b t} (\cosh 2r - 1)} + \frac{2 \cosh 2r [e^{-2\gamma_b t} - e^{-4\gamma_b t}]}{1 + e^{-2\gamma_b t} (\cosh 2r - 1)} \quad (20)$$

The results of Figure 2 (right graph) show, as might be expected, the effect is dominated by the fact that the steering system is damped. Here steering (as measured by  $EPR_{A|B}$ ) is also lost at  $\gamma_b t = \frac{\ln 2}{2}$ .

### E. Decoherence of EPR steering with thermal noise

Now we consider the more complex interaction where there is additional thermal noise for each reservoir. Here we use the full expressions given by Eq. (17). Our results in Figures 3 and 4 reveal several features. We note that the loss of steering is rapid and complete (“sudden-death”) if the thermal noise is placed on the system that is being steered. This effect has been noticed in previous studies of thermal steering and is especially important for asymmetrical systems such as found in opto-mechanics [21, 31, 34, 35]. The effect is more significant as the thermal noise increases, but is reduced for higher  $r$  (Figure 4).

### F. Comparing with the decoherence of entanglement

The effects of the reservoir on the steering are asymmetrical. This will not be true for entanglement: Entanglement is symmetrically defined, with respect to the two different systems involved, and the numerical value we assign to the entanglement will be unchanged under

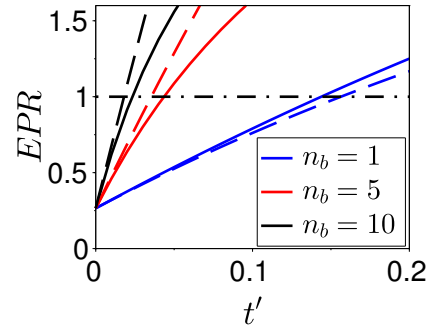


Figure 3. The decoherence of two-mode EPR steering with a thermal reservoir coupled to system  $B$  only. Here  $\gamma_a = 0$ ,  $r = 1$ . We plot the steering signature versus  $t' = \gamma_b t$ . The thermal noise creates a sudden-death type decoherence effect when it is the system that is “being steered” that is coupled to the reservoir. Solid lines correspond to  $EPR_{A|B}$  while dashed lines correspond to  $EPR_{B|A}$ . EPR-steering is obtained when  $EPR < 1$  and the strongest steering is for  $EPR \rightarrow 0$ . We plot different values of  $n_b$ : from bottom to top (for each line type),  $n_b = 1$  (blue),  $n_b = 5$  (red),  $n_b = 10$  (black).

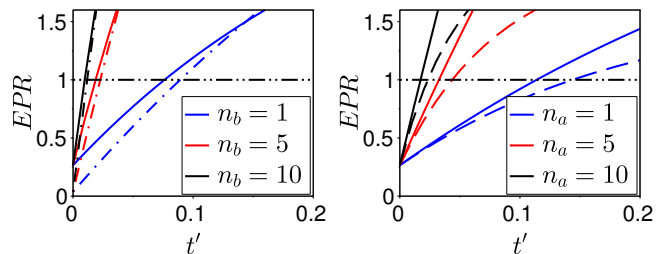


Figure 4. The decoherence of two-mode EPR steering with thermal reservoirs. EPR-steering is obtained when  $EPR < 1$  and the strongest steering is for  $EPR \rightarrow 0$ . **Left graph:** Reservoirs coupled to both systems  $A$  and  $B$  symmetrically. We plot  $EPR_{A|B}$  vs  $t' = \gamma_b t$ . Here  $\gamma_a = \gamma_b$ ,  $n_a = n_b$ ,  $r = 1$ . We plot different values of  $n_b$ , given from bottom to top (for each line type),  $n_b = 1$  (blue),  $n_b = 5$  (red),  $n_b = 10$  (black). Solid lines correspond to  $r = 1$  while dashed-dotted lines correspond to  $r = 2$ . **Right graph:** Thermal reservoir coupling to system  $A$  and cold reservoir coupling to  $B$  ( $\gamma_a = \gamma_b$ ,  $n_a = 1, 5, 10$ ). Solid lines correspond to  $EPR_{A|B}$  while dashed lines correspond to  $EPR_{B|A}$ .

the exchange  $A \leftrightarrow B$ . The relationships between entanglement and EPR steering for Gaussian states have been recently studied [79, 80]. For Gaussian states, it is possible to give a quantification of steering [3, 4, 79, 80], which is an asymmetrical quantum correlation, similar to quantum discord [81–83].

We may evaluate the entanglement via the parameter  $Ent = \Delta(X_A - gX_B)\Delta(P_A + gP_B)/\{1 + g^2\}$  [84, 85]. The inequality  $Ent < 1$  is a necessary and sufficient condition for entanglement of two-mode Gaussian systems for the case we examine here where  $\Delta(X_A - gX_B) =$

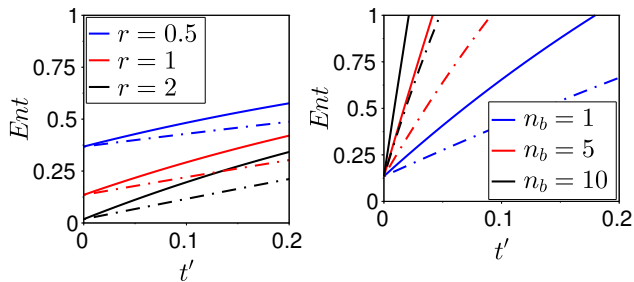


Figure 5. The decoherence of the entanglement of the two-mode squeezed state under the action of a reservoir. The entanglement signature for Gaussian systems  $Ent$  is plotted versus scaled time  $t'$ , under different sorts of reservoir coupling. Entanglement is obtained iff  $Ent < 1$  and stronger entanglement corresponds to  $Ent \rightarrow 0$ . **Left graph:** Here we take all thermal noise zero ( $n_a = n_b = 0$ ). Solid curves show the symmetric case  $\gamma_a = \gamma_b$ . Dashed-dotted curves are for the asymmetric case, for a reservoir coupling to system  $B$  only ( $\gamma_a = 0$ ) when  $t' = \gamma_b t$ ; or, for a reservoir coupling to system  $A$  only ( $\gamma_b = 0$ ) when  $t' = \gamma_a t$ . We plot different values of  $r$ , given from bottom to top (for each line type):  $r = 2$  (black),  $r = 1$  (red),  $r = 0.5$  (blue). **Right graph:** Here we study thermal reservoirs. Solid curves show the symmetric case  $n_a = n_b$  and  $\gamma_a = \gamma_b$ . Dashed-dotted curves are for the asymmetric case, for a reservoir coupling to system  $B$  only ( $\gamma_a = 0$ ) when  $t' = \gamma_b t$ . We plot different values of thermal noise, given from bottom to top (for each line type)  $n_b = 1$  (blue),  $n_b = 5$  (red),  $n_b = 10$  (black).

$\Delta(P_A + gP_B)$ . The condition for optimally chosen  $g$  has been shown equivalent to the Peres-Simon condition in that case [79]. Thus, in this section, we consider the entanglement parameter

$$Ent = \frac{\Delta(X_A - gX_B)\Delta(P_A + gP_B)}{1 + g^2} \quad (21)$$

First we find the value of  $g$  that minimizes the parameter  $Ent$ . We evaluate  $\frac{\partial Ent}{\partial g}$ , in this case we know that  $\Delta(X_A - gX_B) = \Delta(P_A + gP_B)$  hence:

$$\begin{aligned} \frac{\partial Ent}{\partial g} &= \frac{\partial}{\partial g} \frac{\Delta^2(X_A - gX_B)}{1 + g^2} \\ &= \frac{-2\langle X_A X_B \rangle + 2g(\langle X_B^2 \rangle - \langle X_A^2 \rangle) + 2g^2 \langle X_A X_B \rangle}{(1 + g^2)^2} \end{aligned} \quad (22)$$

Next  $\frac{\partial Ent}{\partial g} = 0$ ,

$$\Leftrightarrow -\langle X_A X_B \rangle + g(\langle X_B^2 \rangle - \langle X_A^2 \rangle) + g^2 \langle X_A X_B \rangle = 0$$

Hence the value of  $g$  that minimizes  $Ent$  is [79]:

$$g = \frac{-\langle X_A X_B \rangle + \sqrt{(\langle X_B^2 \rangle - \langle X_A^2 \rangle)^2 + 4\langle X_A X_B \rangle^2}}{2\langle X_A X_B \rangle} \quad (23)$$

We note that if  $\langle X_A^2 \rangle = \langle X_B^2 \rangle$ , then the value of  $g$  that minimises the expression is  $g = 1$ , but where we have asymmetric reservoir effects, like different reservoir couplings or thermal noises, the optimal value will be different to 1. Here we will use from Section II.A that:

$$\begin{aligned} \langle X_A^2 \rangle &= e^{-2\gamma_a t} \cosh 2r + (1 - e^{-2\gamma_a t})(1 + 2n_a) \\ \langle X_A X_B \rangle &= -e^{-(\gamma_a + \gamma_b)t} \sinh 2r \\ \langle X_B^2 \rangle &= e^{-2\gamma_b t} \cosh 2r + (1 - e^{-2\gamma_b t})(1 + 2n_b) \end{aligned} \quad (24)$$

Figure 5 plots the entanglement  $Ent$  for various reservoir couplings. We see from Figure 5 (left graph) that where there is no thermal noise, the entanglement decays steadily, but is never destroyed completely. This effect was noted in [86, 87]. The larger values of  $r$  correspond to larger amounts of entanglement for the initial state before decoherence, and we note that while the decay is sharper for higher  $r$ , a larger initial amount of EPR entanglement will ensure larger EPR entanglement for all later times. The Figure 5 (right graph) shows that when the reservoirs are thermally excited, the entanglement is totally destroyed (in sudden-death fashion) after a finite time. This time is shortened, by increasing the amount of thermal excitation of the reservoir (on either system).

### III. DECOHERENCE OF THE STEERABILITY OF A S-CAT STATE

Traditionally, most studies of decoherence have centred around the Schrodinger cat [45–49]. We noticed in the study of the decoherence of steering for the two-mode squeezed state that for stronger EPR effects, the decay was brought about more sharply, to give overall decoherence times of a similar order (Figure 2). This is consistent with the overall intuition about decoherence in quantum mechanics, that it acts to destroy the more extreme (larger) effects more quickly so that they are not observed in nature. This has been studied for the Schrodinger cat example, where one considers a system initially prepared in superposition of two states macroscopically distinguishable e.g. in phase space [43–49]. The coupling to a reservoir induces a decay of the superposition. Where the separation in phase space increases, calculation and experiments show that the decay rate will increase. Thus, there is an explanation of the transition from microscopic to macroscopic quantum mechanics. Here, motivated by this, we examine the decoherence of the EPR steering of a Schrodinger cat state.

#### A. Steering signature for a Schrodinger cat

Consider the state:

$$|\psi\rangle = \frac{1}{\sqrt{2}}\{|-\alpha\rangle_A |\uparrow\rangle_B + e^{i\theta} |\alpha\rangle_A |\downarrow\rangle_B\} \quad (25)$$



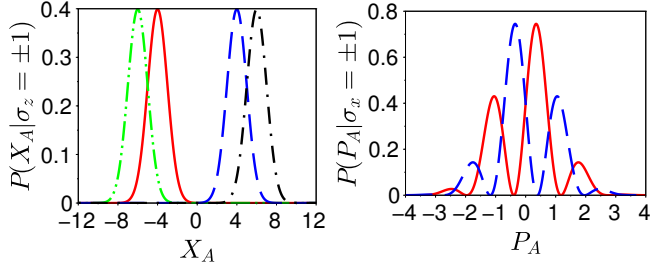


Figure 6. The conditional distributions associated with an EPR steering signature for the Schrodinger cat. **Left Graph:** Conditional probability for  $X_A$  given that the result of a measurement  $\sigma_z$  is  $+1$  (red solid curve is for  $\alpha = 2$ , green dash-dotted curve is for  $\alpha = 3$ ) or  $-1$  (blue long dashed curve is for  $\alpha = 2$ , black short dashed curve is for  $\alpha = 3$ ). **Right Graph:** Conditional probability for  $P_A$  given that the result of the measurement  $\sigma_x$  is  $+1$  (red solid curve) or  $-1$  (blue long dashed curve). Here  $\alpha = 2$ .

which is the entangled Schrodinger cat state. We select  $\theta = \pi/2$  and  $\alpha$  to be real. Here,  $|\alpha\rangle$  is the coherent state for mode  $a$  of system  $A$  and  $|\uparrow\rangle, |\downarrow\rangle$  are the eigenstates of the Pauli spin  $\sigma_z$  of system  $B$ . This state is similar to that described in Schrodinger’s original gedanken experiment [39], where a microscopic system becomes entangled with a macroscopic one, the “cat”. The spin-mode entangled state given by Eq. (25) has been the subject of several experiments [43]. We first explain how one can signify the Schrodinger cat, using EPR steering.

We will derive the probability distributions  $P(X_A)$  (or  $P(P_A)$ ) for the system  $A$ , given that a measurement of the Pauli spin  $\sigma_z$  (or  $\sigma_x$ ) at  $B$  has been carried out to give a result  $+1$  or  $-1$ . We define the scaled amplitudes for position and momentum by  $a = \frac{1}{c}(\hat{x} + i\hat{p})$  where  $a$  is the boson operator, and note that for real position and momentum,  $c = \sqrt{2}$ . In terms of the quadrature phase amplitudes  $X_{A/B}$  and  $P_{A/B}$  defined in Section II, however, we chose the scaling  $c = 2$ . We will distinguish the two cases by using lower and upper case, respectively, and note we have dropped the use of the operator hats where the meaning is clear, or to denote the outcomes of the measurements. As expected from direct examination of the state (25), the distributions  $P(x|+1)$  and  $P(x|-1)$  for the result  $x$  at  $A$  given the outcomes  $+1$  or  $-1$  for  $\sigma_z$  at  $B$ , are the two Gaussian hills (Figure 6, left graph): Specifically,

$$P\left(x|\sigma_z = \pm 1\right) = \left(\frac{2}{\pi}\right)^{\frac{1}{2}} \frac{1}{c} \exp\left[-2\frac{x^2}{c^2} - 2\alpha^2 \mp 4\frac{x\alpha}{c}\right] \quad (26)$$

Next, we derive the conditional distributions for  $P(P_A)$  given that a measurement of Pauli spin  $\sigma_x$  at  $B$  yields the result  $+1$  or  $-1$ . To evaluate this, we rewrite the state in terms of the basis states  $|\uparrow\rangle_x$  and  $|\downarrow\rangle_x$  for the

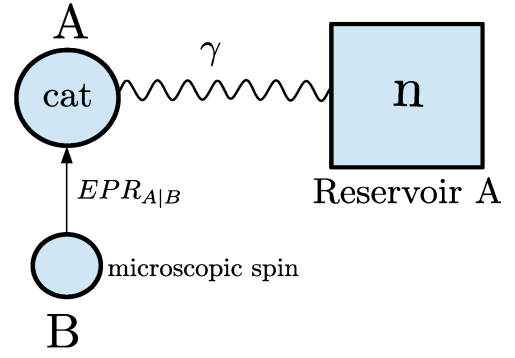


Figure 7. The steering of a Schrodinger cat. We have proposed a signature for the cat, based on EPR steering parameter  $EPR_{A|B}$ . Here, measurements made on the microscopic spin system  $B$  “steer” the macroscopic system (the cat)  $A$ . The “cat” in this case is modelled as the superposition involving two coherent states,  $|\alpha\rangle$  and  $|\alpha\rangle$ . The value of  $\alpha$  determines the size of the Schrodinger cat. We consider that the “cat” being macroscopic is coupled to a thermal reservoir. We examine the decay of the steering signature, with respect to the parameters of the reservoir coupling.

spin  $\sigma_x$ .

$$|\psi\rangle = \frac{1}{2}(|-\alpha\rangle_A + i|\alpha\rangle_A)|\uparrow\rangle_{x,B} + \frac{1}{2}(i|\alpha\rangle_A - |-\alpha\rangle_A)|\downarrow\rangle_{x,B} \quad (27)$$

At this point, we note the for other choices of  $\theta$ , normalisation factors are more complicated. We find that the probability for the momentum given the results for spin  $\sigma_x$  is

$$P\left(p|\sigma_x = \pm 1\right) = \left(\frac{2}{\pi}\right)^{\frac{1}{2}} \frac{1}{c} e^{-2\frac{p^2}{c^2}} \left(1 \pm \sin\left(4\frac{p\alpha}{c}\right)\right) \quad (28)$$

This allows us to calculate the conditional variances that give us a signature for EPR steering. An EPR steering of the “cat” is observed when

$$EPR = Var(X_A|\sigma_z)Var(P_A|\sigma_x) < 1 \quad (29)$$

where here

$$Var(X_A|\sigma_z) = P_z(+1)Var(X_A|+1) + P_z(-1)Var(X_A|-1)$$

denotes the conditional variance for  $X_A$  averaged over the outcomes of  $\sigma_z$ . We have used the notation  $Var(X_A|\pm 1)$  to mean the variance of  $P(X_A|\pm 1)$ , which is the probability distribution for  $X_A$  given the outcome  $\pm 1$  for the measurement  $\sigma_z$ , respectively. The  $Var(P_A|\sigma_x)$  is defined similarly, but for outcomes of  $\sigma_x$ . The right-side bound is the quantum noise limit, as determined by the Heisenberg uncertainty relation which in this case for the

choice  $c = 2$  is  $\Delta X_B \Delta P_B \geq 1$ . We note that the derivation of the inequality as a signature of EPR steering has been given in the Refs. [5, 15, 16].

The EPR quantity (29) can be evaluated: We see that for the two Gaussian hills, the variance is at the quantum noise level (Figure 6, left graph):  $\text{Var}(X_A | \sigma_z) = 1$ . On the other hand, the variance associated with the momentum distributions is reduced below 1 (Figure 6, right graph), implying that  $EPR_{A|B} < 1$ . We can calculate the variance from the conditional distributions. Alternatively, noting that the collapsed state for system  $B$  given a measurement  $\sigma_x$  is the superposition  $\frac{1}{2}(|-\alpha\rangle_A + i|\alpha\rangle_A)$  (for result  $+1$ ) or  $\frac{1}{2}(i|\alpha\rangle_A - |-\alpha\rangle_A)$  (for result  $-1$ ), it is easy to use the methods and results of the next section, to find that

$$\text{Var}(P_A | \sigma_x) = 1 - 4\alpha^2 e^{-4|\alpha|^2} \quad (30)$$

The steering inequality (29) has been suggested in Ref. [54], as a way to realise an EPR paradox with the Schrodinger cat state. The steering cannot be obtained if the system is in the *mixture of states*,  $|-\alpha\rangle_A | \uparrow \rangle_B$  and  $|\alpha\rangle_A | \downarrow \rangle_B$ , that allows a classical dead *or* alive description. This case is especially interesting, because it focuses on the steering of a *mesoscopic* system (the Schrodinger cat) [34]. If we assume Local Realism is valid, then it is the local state of the mesoscopic system that is shown to be inconsistent with the quantum mechanics (refer to the LHS model of the Section II.B). This contrasts with EPR's original argument, which showed the inconsistency for a *microscopic* system [7].

### B. Decoherence of the Schrodinger cat with a heat bath

It will prove useful to next study the interaction of the single mode ‘‘Schrodinger cat’’ state [45–48]

$$|\psi\rangle = \frac{1}{\sqrt{2}}\{ |-\alpha\rangle + i|\alpha\rangle \} \quad (31)$$

with a reservoir. This was analysed by many authors, including Yurke and Stoler [45–49]. We consider that the single mode, prepared in the Schrodinger cat state, is then coupled to a thermal heat bath with dissipation. Using the solutions from Section II.C, we can calculate the moments at a later time  $t$ , in terms of the initial moments:

$$\langle a^\dagger(t)a(t) \rangle = e^{-2\gamma t} \langle a^\dagger(0)a(0) \rangle + n(1 - e^{-2\gamma t})$$

$$\langle a(t)a(t) \rangle = e^{-2\gamma t} \langle a(0)a(0) \rangle$$

Denoting the variances using shorthand notation, by  $\Delta^2 P = (\Delta P)^2$  and  $\Delta^2 X = (\Delta X)^2$ , we find

$$\Delta^2 P = 1 + 2n(1 - e^{-2\gamma t}) - 4\alpha^2 e^{-2\gamma t} e^{-4\alpha^2} \quad (32)$$

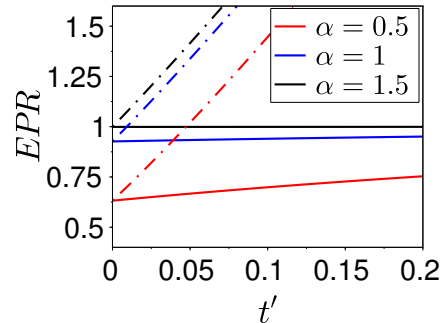


Figure 8. The decoherence of the Schrodinger cat EPR-steering signature  $EPR$  for the system depicted in Fig. 7. Here, a thermal reservoir is coupled to the spin system  $B$ . We plot the steering signature versus  $t' = \gamma t$ . Here we consider different sizes of the ‘‘cat’’ (solid line lower to top,  $\alpha = 0.5, 1$  and  $1.5$ ). For each  $\alpha$ , we plot different values of  $n$ :  $n = 0$  (solid),  $n = 1$  (dashed-dotted).

We see that the variance for  $P$  can be reduced below the quantum limit (given by 1). The reduction of the variance of  $P$  below the quantum limit is in itself a signature for the ‘‘cat’’ state. We see this as follows. If we take  $\alpha$  large, and assume no thermal noise and  $\gamma = 0$ , then the probability distribution  $P(x)$  associated with each of the ‘‘dead’’ and ‘‘alive’’ states is a Gaussian hill, with variance 1. If the system were to actually be in any kind of mixture of these quantum states, then the variance for  $P$  could not drop below 1 because of the uncertainty relation (and the fact that mixing states cannot decrease the variance) [54, 88]. The observation of a reduced variance for  $P$  can thus occur for a superposition *but not for a mixture* of the two quantum states that possess a distribution  $P(x)$  given by the Gaussian hills. The details are not studied further here however, since our objective is to study the decoherence of steering.

### C. Decoherence of the steering of the Schrodinger cat

Motivated by this, we now examine the decoherence of the EPR steering of a Schrodinger cat state, as given by the signature Eq. (29). We consider the two-mode case where  $A$  is a harmonic oscillator coupled to a heat bath from time  $t = 0$  and the second system is the spin  $B$  (no heat bath coupling), as depicted in Figure 7. The system is *prepared* in the entangled Schrodinger cat state

$$|\psi\rangle = \frac{1}{\sqrt{2}}\{ |-\alpha\rangle_A | \uparrow \rangle_B + i|\alpha\rangle_A | \downarrow \rangle_B \} \quad (33)$$

We can rewrite this state in terms of the basis states  $| \uparrow \rangle_x$  and  $| \downarrow \rangle_x$  for the spin  $\sigma_x$  as shown in Section III.A. It is straightforward to calculate the moments  $\langle a\sigma_z \rangle$ ,  $\langle a^2\sigma_z \rangle$ , etc. at the time  $t = 0$ . The moments at a later time  $t$



(after the interaction with the heat bath has been turned on) can be evaluated using the solution (12) of Section II.C. We note that since the reservoir interaction does not involve the spins, we have  $\sigma_z(t) = \sigma_z(0)$ ,  $\sigma_x(t) = \sigma_x(0)$ . Therefore, we can calculate the moments at the time  $t$ , in terms of the moments at the initial time  $t = 0$ .

We next consider the moments of the distributions at the time  $t$  for  $X_A$  and  $P_A$ , *conditional* on getting the result either  $+1$  or  $-1$  for the Pauli spin measurement on  $B$ . These moments can be readily calculated. We outline the method. We use the notation, for example,  $\langle X_A | 1 \rangle_z$  to denote the moment  $\langle X_A \rangle$  of system  $A$ , conditioned on the result  $+1$  for spin  $\sigma_z$  at  $B$ . Let us suppose then that we obtain the outcomes  $X_A$  at  $A$ , and  $\sigma_z$  at  $B$ . We define the measurable probability  $P(X_A, \sigma_z)$  for the joint outcomes. We see that:  $P(X_A | \sigma_z) = \frac{P(X_A, \sigma_z)}{P_z(\sigma_z)}$ . It follows that  $P(X_A, \pm 1) = P(X_A | \pm 1)P_z(\pm 1) = \frac{1}{2}P(X_A | \pm 1)$ . Hence,  $\langle X_A \sigma_z \rangle = P(X_A, 1)X_A - P(X_A, -1)X_A = P(X_A | 1)P_z(1)X_A - P(X_A | -1)P_z(-1)X_A = \frac{1}{2}\{\langle X_A | 1 \rangle - \langle X_A | -1 \rangle\}$ . Following this procedure, we see that:

$$\begin{aligned} \langle X_A \sigma_z \rangle &= \frac{1}{2}\{\langle X_A | 1 \rangle_z - \langle X_A | -1 \rangle_z\} \\ \langle X_A \rangle &= \frac{1}{2}\{\langle X_A | 1 \rangle_z + \langle X_A | -1 \rangle_z\} \end{aligned} \quad (34)$$

and similarly for the moments involving  $X_A^2$ . This allows us to solve for the conditional moments using the relations such as  $\langle X_A | 1 \rangle_z = \langle X_A \sigma_z \rangle + \langle X_A \rangle$  and  $\langle X_A | -1 \rangle_z = -\langle X_A \sigma_z \rangle + \langle X_A \rangle$ . We also define the same relations, but replacing  $X_A$  with  $P_A$  and  $\sigma_z$  with  $\sigma_x$ . The final solutions for the conditional moments are:  $\langle X_A | \pm 1 \rangle_z = \mp 2\alpha e^{-\gamma t}$ ,  $\langle X_A^2 | \pm 1 \rangle_z = 1 + 2n(1 - e^{-2\gamma t}) + 4\alpha^2 e^{-2\gamma t}$ ,  $\langle P_A | \pm 1 \rangle_x = \mp 2\alpha e^{-\gamma t} e^{-2\alpha^2}$  and  $\langle P_A^2 | \pm 1 \rangle_x = 1 + 2n(1 - e^{-2\gamma t})$ . Hence we solve for the average variance  $Var(X_A | \sigma_z)$  of  $X$  conditioned on the measurement of spin  $\sigma_z$  at  $B$ : We obtain

$$Var(X_A | \sigma_z) = 1 + 2n(1 - e^{-2\gamma t}) \quad (35)$$

Similarly, we can solve for variance  $Var(P_A | \sigma_x)$  of  $P_A$  conditioned on spin  $\sigma_x$  at  $B$ , to obtain

$$Var(P_A | \sigma_x) = 1 + 2n(1 - e^{-2\gamma t}) - 4\alpha^2 e^{-2\gamma t} e^{-4\alpha^2} \quad (36)$$

To show how the EPR steering signature decoheres with time, we evaluate

$$EPR = Var(X_A | \sigma_z) Var(P_A | \sigma_x) \quad (37)$$

Here, we use the notation defined in Section III.A.

We find that with  $n = 0$  (no thermal noise), the value of  $EPR$  is identical to that of  $Var(P_A | \sigma_x)$ , which is also identical to the variance  $\Delta^2 P$  given by Eq. (32). This value is plotted in Figure 8 (solid lines). By the above argument, the signature of the S-cat is the drop below 1 of  $EPR$ . We note that as  $\alpha$  increases, the  $EPR$  value tends to 1, the signature therefore becoming more sensitive to decoherence. This reduction in variance of  $P$  as  $\alpha$  increases is directly associated with the interference fringes in the distribution  $P(P_A)$  [45–48]. These fringes become finer as  $\alpha$  increases, as evident from the function given by Eq. (28). With thermal noise, we see that the value of  $EPR$  increases: a much greater sensitivity to decoherence is apparent, as illustrated in Figure 8 by the dashed-dotted curves.

#### IV. CONCLUSION

The directional properties of EPR steering are significant when it comes to understanding the decoherence of EPR-steering. We have shown how when two systems are coupled independently to a reservoir, the steering is asymmetrically affected. If we consider the steering of a system  $A$  by measurements made on the system  $B$ , then the steering is sensitive to the reservoir coupling to system  $B$ . This is intuitively not surprising, given the Local Hidden State (LHS) definition of EPR steering as a nonlocality. In terms of the LHS description that is to be negated in order to confirm such steering by B [3, 4], it is the hidden states of system  $B$  that are like those considered by Bell. The sensitivity of the steering to the losses on the system  $B$  has been studied experimentally, in the context of the EPR paradox [54, 86, 87]. There, it was known that the EPR criterion could not be achieved, with 50% or more losses on the steering system  $A$ . Recent work considers this result in terms of the monogamy properties of EPR steering [59]. The sensitivity of the steering signatures to losses (which may represent an eavesdropper on the channel) has potentially important implications for quantum cryptography [64, 68].

The behaviour with respect to the thermal noise appears almost reversed. This has implications for detecting steering of Schrodinger cats which are coupled to hot reservoirs. For the Schrodinger cat example, we explained how the steering acts as a signature of the Schrodinger cat. Adding thermal noise to the system  $B$  significantly affects the amount of EPR steering of system  $A$ . There have been recent theoretical studies of the steering of a mechanical oscillator, which we liken to a “cat”, by measurements made on an optical pulse [34, 35]. In those studies, the thermal noise of the oscillator was shown to have a quite dramatic effect on the amount of steering possible. By comparison, the entanglement between the thermal oscillator and the pulse was quite robust. Similar results have been obtained for Bose Ein-

stein condensates [31]. These results are consistent with the simple descriptions of decoherence given in this paper.

### ACKNOWLEDGMENTS

This work was supported by an Australian Research Council Discovery Project Grant. We are grateful to B.

Dalton for many helpful suggestions.

- 
- [1] E. Schrodinger, "Discussion of probability relations between separated systems," *Proc. Cambridge Philos. Soc.* **31**, 555-563 (1935).
- [2] E. Schrodinger, "Probability relations between separated systems," *Proc. Cambridge Philos. Soc.* **32**, 446-452 (1936).
- [3] H. M. Wiseman, S. J. Jones, and A. C. Doherty, "Steering, entanglement, nonlocality, and the Einstein-Podolsky-Rosen paradox," *Phys. Rev. Lett.* **98**, 140402 (2007).
- [4] S. J. Jones, H. M. Wiseman, and A. C. Doherty, "Entanglement, Einstein-Podolsky-Rosen correlations, Bell nonlocality, and steering," *Phys. Rev. A* **76**, 052116 (2007).
- [5] E. G. Cavalcanti, S. J. Jones, H. M. Wiseman, and M. D. Reid, "Experimental criteria for steering and the Einstein-Podolsky-Rosen paradox," *Phys. Rev. A* **80**, 032112 (2009).
- [6] D. J. Saunders, S. J. Jones, H. M. Wiseman, and G. J. Pryde, "Experimental EPR-steering using Bell-local states," *Nature Physics* **6**, 845-849 (2010).
- [7] A. Einstein, B. Podolsky and N. Rosen, "Can quantum-mechanical description of physical reality be considered complete?," *Phys. Rev.* **47**, 777-780 (1935).
- [8] J. S. Bell, "Speakable and unspeakable in quantum mechanics" (Cambridge University Press, Cambridge, 1987).
- [9] J. S. Bell, "On the Einstein-Podolsky-Rosen paradox," *Physics* **1**, 195-200 (1964).
- [10] J. F. Clauser, M. A. Horne, A. Shimony, and R. A. Holt, "Proposed experiment to test local hidden-variable theories," *Phys. Rev. Lett.* **23**, 880-884 (1969).
- [11] M. Giustina, A. Mech, S. Ramelow, B. Wittmann, J. Kofler, J. Beyer, A. Lita, B. Calkins, T. Gerrits, S. W. Nam, R. Ursin, and A. Zeilinger, "Bell violation using entangled photons without the fair-sampling assumption," *Nature* **497**, 227-230 (2013).
- [12] B. G. Christensen, K. T. McCusker, J. B. Altepeter, B. Calkins, T. Gerrits, A. E. Lita, A. Miller, L. K. Shalm, Y. Zhang, S. W. Nam, N. Brunner, C. C. W. Lim, N. Gisin, and P. G. Kwiat, "Detection-loophole-free test of quantum nonlocality, and applications," *Phys. Rev. Lett.* **111**, 130406 (2013).
- [13] C. S. Wu, and I. Shaknov, "The angular correlation of scattered annihilation radiation," *Physical Review A* **77**, 136 (1950).
- [14] Z. Y. Ou, S. F. Pereira, H. J. Kimble, and K. C. Peng, "Realization of the Einstein-Podolsky-Rosen paradox for continuous variables," *Phys. Rev. Lett.* **68**, 3663-3666 (1992).
- [15] M. D. Reid, P. D. Drummond, W. P. Bowen, E. G. Cavalcanti, P. K. Lam, H. A. Bachor, U. L. Andersen, and G. Leuchs, "Colloquium: The Einstein-Podolsky-Rosen paradox: From concepts to applications," *Rev. Mod. Phys.* **81**, 1727-1751 (2009).
- [16] M. D. Reid, "Demonstration of the Einstein-Podolsky-Rosen paradox using nondegenerate parametric amplification," *Phys. Rev. A* **40**, 913-923 (1989).
- [17] M. D. Reid, and P. D. Drummond, "Quantum correlations of phase in nondegenerate parametric oscillation," *Phys. Rev. Lett.* **60**, 2731-2733 (1988).
- [18] K. Dechoum, S. Chaturvedi, P. Drummond, and M. D. Reid, "Critical fluctuations and entanglement in the nondegenerate parametric oscillator," *Phys. Rev. A* **70**, 053807 (2004).
- [19] B. Julsgaard, A. Kozhekin, and E. S. Polzik, "Experimental long-lived entanglement of two macroscopic objects," *Nature* **413**, 400-403 (2001).
- [20] H. Krauter, C. A. Muschik, K. Jensen, W. Wasilewski, J. M. Petersen, J. I. Cirac, and E. S. Polzik, "Entanglement generated by dissipation and steady state entanglement of two macroscopic objects," *Phys. Rev. Lett.* **107** 080503 (2011).
- [21] Q. He, and M. Reid, "Towards an Einstein-Podolsky-Rosen paradox between two macroscopic atomic ensembles at room temperature," *New J. Phys.*, **15**, 063027 (2013).
- [22] C. Gross, H. Strobel, E. Nicklas, T. Zibold, N. Bar-Gill, G. Kurizki, and M. K. Oberthaler, "Atomic homodyne detection of continuous-variable entangled twin-atom states," *Nature* **480**, 219-233 (2011).
- [23] N. Bar-Gill, C. Gross, I. Mazets, M. Oberthaler, and G. Kurizki, "Einstein-Podolsky-Rosen correlations of ultracold atomic gases," *Phys. Rev. Lett.* **106**, 120404 (2011).
- [24] K. Kheruntsyan, M. Olsen, and P. D. Drummond, "Einstein-Podolsky-Rosen correlations via dissociation of a molecular Bose-Einstein condensate," *Phys. Rev. Lett.* **95**, 150405 (2005).
- [25] M. Ögren, and K. V. Kheruntsyan, "Role of spatial inhomogeneity in dissociation of trapped molecular condensates," *Phys. Rev. A* **82**, 013641 (2010).
- [26] J. Jaskula, M. Bonneau, G. B. Partridge, V. Krachmalnicoff, P. Deuar, K. V. Kheruntsyan, A. Aspect, D. Boiron, and C. I. Westbrook, "Sub-Poissonian number differences in four-wave mixing of matter waves," *Phys. Rev. Lett.* **105**, 190402 (2010).
- [27] A. Ferris, M. Olsen, E. Cavalcanti, and M. Davis, "Detection of continuous variable entanglement without coherent local oscillators," *Phys. Rev. A* **78**, 060104 (2008).
- [28] Q. He, M. Reid, T. Vaughan, C. Gross, M. Oberthaler, and P. Drummond, "Einstein-Podolsky-Rosen entangle-

- ment strategies in two-well Bose-Einstein condensates,” *Phys. Rev. Lett.* **106**, 120405 (2011).
- [29] Q. He, P. Drummond, M. Olsen, and M. D. Reid, “Einstein-Podolsky-Rosen entanglement and steering in two-well Bose-Einstein-condensate ground states,” *Phys. Rev. A* **86**, 023626 (2012)
- [30] B. Opanchuk, Q. He, M. Reid, and P. Drummond, “Dynamical preparation of Einstein-Podolsky-Rosen entanglement in two-well Bose-Einstein condensates,” *Phys. Rev. A* **86**, 023625 (2012).
- [31] R. J. Lewis-Swan, and K. V. Kheruntsyan, “Sensitivity to thermal noise of atomic Einstein-Podolsky-Rosen entanglement,” *Phys. Rev. A* **87**, 063635 (2013).
- [32] S. G. Hofer, W. Wieczorek, M. Aspelmeyer, and K. Hammerer, “Quantum entanglement and teleportation in pulsed cavity optomechanics,” *Phys. Rev. A* **84**, 052327 (2011).
- [33] V. Giovannetti, S. Mancini, and P. Tombesi, “Radiation pressure induced Einstein-Podolsky-Rosen paradox,” *Europhys. Lett.* **54**, 559-565 (2001).
- [34] Q. He, and M. Reid, “Einstein-Podolsky-Rosen paradox and quantum steering in pulsed optomechanics,” *Phys. Rev. A* **88**, 052121 (2013).
- [35] S. Kiesewetter, Q. Y. He, P. D. Drummond, and M. D. Reid, “Scalable quantum simulation of pulsed entanglement and Einstein-Podolsky-Rosen steering in optomechanics,” *Phys. Rev. A* **90**, 043805 (2014).
- [36] B. Wittmann, S. Ramelow, F. Steinlechner, N. K. Langford, N. Brunner, H. M. Wiseman, R. Ursin, and A. Zeilinger, “Loophole-free Einstein-Podolsky-Rosen experiment via quantum steering,” *New J. Phys.* **14**, 053030 (2012).
- [37] D. Smith, G. Gillett, M. P. de Almeida, C. Branciard, A. Fedrizzi, T. J. Weinhold, A. Lita, B. Calkins, T. Gerrits, H. M. Wiseman, S. W. Nam, and A. G. White, “Conclusive quantum steering with superconducting transition-edge sensors,” *Nature Communications* **3**, 625-630 (2012).
- [38] A. J. Bennett, D. A. Evans, D. J. Saunders, C. Branciard, E. G. Cavalcanti, H. M. Wiseman, and G. J. Pryde, “Arbitrarily loss-tolerant Einstein-Podolsky-Rosen steering allowing a demonstration over 1 km of optical fiber with no detection loophole,” *Physical Review X* **2**, 031003 (2012).
- [39] E. Schroedinger, “Die gegenwärtige situation in der quantenmechanik,” *Naturwiss.* **23**, 807-812 (1935).
- [40] D. Leibfried, E. Knill, S. Seidelin, J. Britton, R. B. Blakestad, J. Chiaverini, D. B. Hume, W. M. Itano, J. D. Jost, C. Langer, R. Ozeri, R. Reichle, and D. J. Wineland, “Creation of a six-atom ‘Schrödinger cat’ state,” *Nature*, **438**, 639-642 (2005).
- [41] T. Monz, P. Schindler, J. T. Barreiro, M. Chwalla, D. Nigg, W. A. Coish, M. Harlander, W. Hänsel, M. Hennrich, and R. Blatt, “14-qubit entanglement: Creation and coherence,” *Phys Rev Lett* **106**, 130506 (2011).
- [42] A. Ourjoumtsev, R. Tualle-Broui, J. Laurat, and P. Grangier, “Generating optical Schrödinger kittens for quantum information processing,” *Science* **312**, 83-86, (2006).
- [43] M. Brune, E. Hagley, J. Dreyer, X. Maître, A. Maali, C. Wunderlich, J. M. Raimond, and S. Haroche, “Observing the progressive decoherence of the ‘meter’ in a quantum measurement,” *Phys. Rev. Lett.* **77**, 4887-4890 (1996).
- [44] C. Monroe, D. M. Meekhof, B. E. King, and D. J. Wineland, “A ‘Schrödinger Cat’ superposition state of an atom,” *Science* **272**, 1131-1136 (1996).
- [45] B. Yurke, and D. Stoler, “Generating quantum mechanical superpositions of macroscopically distinguishable states via amplitude dispersion,” *Phys. Rev. Lett.* **57**, 13-16 (1986).
- [46] A. Gilchrist and W. J. Munro, “Signatures of the pair-coherent state,” *J. Opt. B* **2** 47-52 (2000).
- [47] G. Milburn, and C. Holmes, “Dissipative quantum and classical Liouville mechanics of the anharmonic oscillator,” *Phys. Rev. Lett.* **56**, 2237-2240 (1986).
- [48] A. Dragan, and K. Banaszek, “Homodyne Bell’s inequalities for entangled mesoscopic superpositions,” *Phys. Rev. A* **63**, 062102 (2001).
- [49] A. Caldeira, and A. J. Leggett, “Influence of dissipation on quantum tunneling in macroscopic systems,” *Phys. Rev. Lett.*, **46**, 211-214, (1981).
- [50] S. Armstrong, M. Wang, R. Y. Teh, Q. Gong, Q. He, J. Janousek, Hans-Albert Bachor, M. D. Reid, and P. K. Lam, “Multipartite Einstein-Podolsky-Rosen steering and genuine tripartite entanglement with optical networks,” *Nat. Phys.* **11**, 167-172 (2015).
- [51] Q. Y. He, and M. D. Reid, “Genuine multipartite Einstein-Podolsky-Rosen steering,” *Phys Rev Lett.* **111**, 250403 (2013).
- [52] D. Cavalcanti, P. Skrzypczyk, G. H. Aguilar, R. V. Nery, P. H. Souto Ribeiro, and S. P. Walborn, “Detecting multipartite entanglement with untrusted measurements in asymmetric quantum networks,” *arXiv:1412.7730v2* (2014).
- [53] C. M. Li, K. Chen, Y. Chen, Q. Zhang, Y. Chen, J. W. Pan, “Genuine high-order Einstein-Podolsky-Rosen steering,” *arXiv:1501.01452* (2015).
- [54] E. G. Cavalcanti, and M. D. Reid, “Criteria for generalized macroscopic and mesoscopic quantum coherence,” *Phys. Rev. A* **77**, 062108 (2008).
- [55] S. L. W. Midgley, A. J. Ferris, and M. K. Olsen, “Asymmetric Gaussian steering: When Alice and Bob disagree,” *Phys. Rev. A* **81**, 022101 (2010).
- [56] V. Händchen, T. Eberle, S. Steinlechner, A. Sambrowski, T. Franz, R. F. Werner, and R. Schnabel, “Observation of one-way Einstein-Podolsky-Rosen steering,” *Nature Photonics* **6**, 598-601 (2012).
- [57] S. P. Walborn, A. Salles, R. M. Gomes, F. Toscano, and P. H. Souto Ribeiro, “Revealing hidden Einstein-Podolsky-Rosen nonlocality,” *Phys. Rev. Lett.* **106**, 130402 (2011).
- [58] J. Schneeloch, C. J. Broadbent, S. P. Walborn, E. G. Cavalcanti, and J. C. Howell, “Einstein-Podolsky-Rosen steering inequalities from entropic uncertainty relations,” *Phys. Rev. A* **87**, 062103 (2013).
- [59] M. D. Reid, “Monogamy inequalities for the Einstein-Podolsky-Rosen paradox and quantum steering,” *Phys. Rev. A* **88**, 062108 (2013).
- [60] J. Bowles, T. Vértesi, M. T. Quintino, and N. Brunner, “One-way Einstein-Podolsky-Rosen steering,” *Phys. Rev. Lett.* **112**, 200402 (2014).
- [61] T. C. Ralph, “Continuous variable quantum cryptography,” *Phys. Rev. A* **61**, 010303(R) (1999).
- [62] M. D. Reid, “Quantum cryptography with a predetermined key, using continuous-variable Einstein-Podolsky-Rosen correlations,” *Phys. Rev. A* **62**, 062308 (2000).
- [63] M. D. Reid, in “Quantum Squeezing” editors P. D. Drummond, and Z. Ficek (Springer, 2004), p. 337.

- [64] C. Branciard, E. G. Cavalcanti, S. P. Walborn, V. Scarani, and H. M. Wiseman, “One-sided device-independent quantum key distribution: Security, feasibility, and the connection with steering,” *Phys. Rev. A* **85**, 010301(R) (2012).
- [65] F. Grosshans, and P. Grangier, “Quantum cloning and teleportation criteria for continuous quantum variables,” *Phys. Rev. A* **64**, 010301(R) (2001).
- [66] X. Ma, and N. Lutkenhaus, “Improved data post-processing in quantum key distribution and application to loss thresholds in device independent QKD,” *Quantum Inf. Comput.* **12**, 203-214 (2012).
- [67] M. D. Reid, “Signifying quantum benchmarks for qubit teleportation and secure quantum communication using Einstein-Podolsky-Rosen steering inequalities,” *Phys. Rev. A* **88**, 062338 (2013).
- [68] B. Opanchuk, L. Arnaud, and M. D. Reid, “Detecting faked continuous-variable entanglement using one-sided device-independent entanglement witnesses,” *Phys. Rev. A* **89**, 062101 (2014).
- [69] B. L. Schumaker, and C. M. Caves, “New formalism for two-photon quantum optics. II. Mathematical foundation and compact notation,” *Phys. Rev. A* **31**, 3093-3111 (1985).
- [70] A. Furusawa, J. L. Sørensen, S. L. Braunstein, C. A. Fuchs, H. J. Kimble, and E. S. Polzik, “Unconditional quantum teleportation,” *Science* **282**, 706-709 (1998).
- [71] A. Heidmann, R. J. Horowicz, S. Reynaud, E. Giacobino, C. Fabre, and G. Camy, “Observation of quantum noise reduction on twin laser beams,” *Phys Rev. Lett.* **59**, 2555-2557 (1987).
- [72] A. S. Lane, M. D. Reid, and D. F. Walls, “Absorption spectroscopy beyond the shot-noise limit,” *Phys Rev Lett.* **60**, 1940-1942 (1988).
- [73] C. Weedbrook, S. Pirandola, R. García-Patrón, N. J. Cerf, T. C. Ralph, J. H. Shapiro, and S. Lloyd, “Gaussian quantum information,” *Rev. Mod. Phys.* **84**, 621-669 (2012).
- [74] C. W. Gardiner, and M. Collett, “Input and output in damped quantum systems: Quantum stochastic differential equations and the master equation,” *Phys. Rev. A* **31**, 3761-3774 (1985).
- [75] M. J. Collett, and C. Gardiner, “Squeezing of intracavity and traveling-wave light fields produced in parametric amplification,” *Phys. Rev. A* **30**, 1386-1391 (1984).
- [76] T. Yu, and J. H. Eberly, “Finite-time disentanglement via spontaneous emission,” *Phys. Rev. Lett.* **93**, 140404 (2004)
- [77] M. P. Almeida, F. de Melo, M. Hor-Meyll, A. Salles, S. P. Walborn, P. H. Souto Ribeiro, and L. Davidovich, “Environment-induced sudden death of entanglement,” *Science* **316**, 579-582 (2007).
- [78] S. Chan, M. D. Reid, and Z. Ficek, “Entanglement evolution of two remote and non-identical Jaynes-Cummings atoms,” *J. Phys. B: At. Mol. Opt. Phys.* **42**, 065507 (2009).
- [79] Q. Y. He, Q. H. Gong, and M. D. Reid, “Classifying directional Gaussian entanglement, Einstein-Podolsky-Rosen steering, and discord,” *Phys. Rev. Lett.* **114**, 060402 (2015).
- [80] I. Kogias, A. R. Lee, S. Ragy, and G. Adesso, “Quantification of Gaussian quantum steering,” *Phys. Rev. Lett.* **114**, 060403 (2015).
- [81] P. Giorda and M. G. A. Paris, “Gaussian Quantum Discord”, *Phys. Rev. Lett.* **105**, 020503 (2010).
- [82] G. Adesso and A. Datta, “Quantum versus Classical Correlations in Gaussian states”, *Phys. Rev. Lett.* **105**, 030501 (2010).
- [83] S. Pirandola, G. Spedalieri, S. L. Braunstein, N. J. Cerf, and S. Lloyd, "Optimality of Gaussian Discord", *Phys. Rev. Lett.* **113**, 140405 (2014).
- [84] L. M. Duan, G. Giedke, J. I. Cirac, and P. Zoller, “Inseparability criterion for continuous variable systems,” *Phys. Rev. Lett.* **84**, 2722-2725 (2000).
- [85] V. Giovannetti, S. Mancini, D. Vitali, and P. Tombesi, “Characterizing the entanglement of bipartite quantum systems,” *Phys. Rev. A* **67**, 022320 (2003).
- [86] D. Buono, G. Nocerino, A. Porzio, and S. Solimeno, “Experimental analysis of decoherence in continuous-variable bipartite systems,” *Phys. Rev. A* **86**, 042308 (2012).
- [87] W. P. Bowen, R. Schnabel, P. K. Lam, and T. C. Ralph, “Experimental Investigation of Criteria for Continuous Variable Entanglement,” *Phys. Rev. Lett.* **90**, 043601 (2003).
- [88] E. G. Cavalcanti, and M.D. Reid, “Signatures for generalized macroscopic superpositions,” *Phys. Rev. Lett.* **97**, 170405 (2006).